

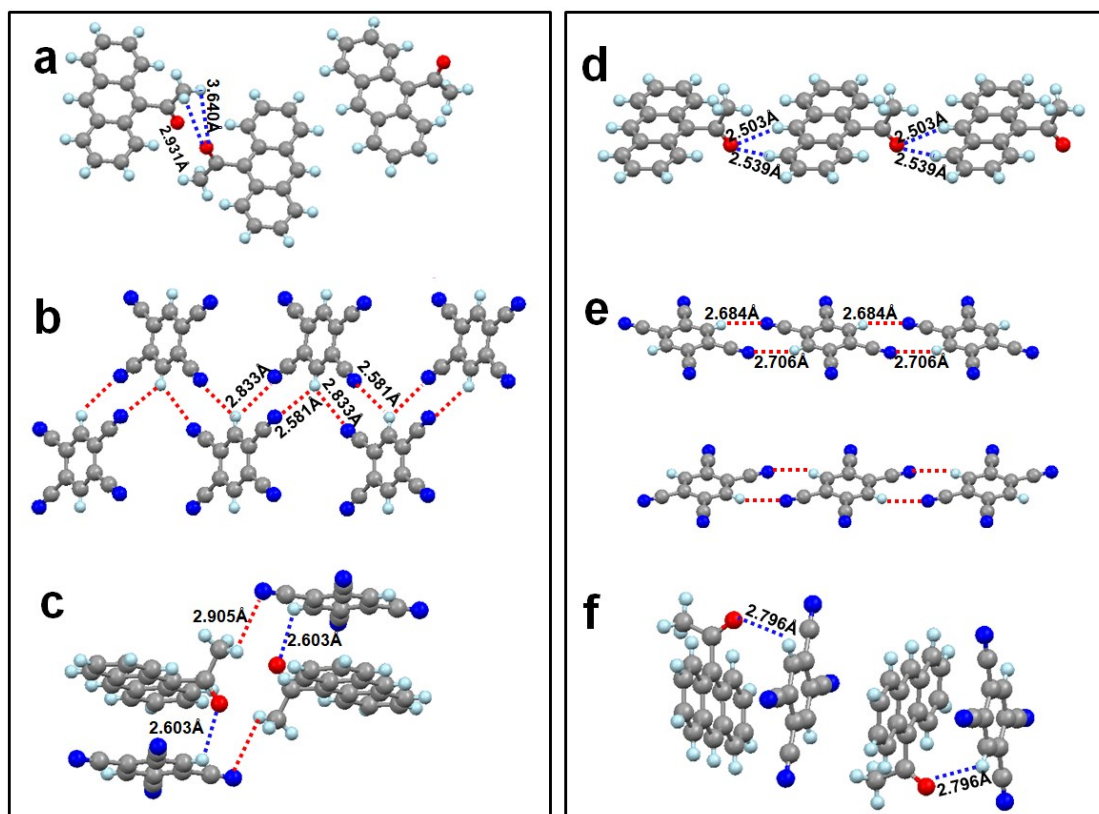
## Supporting Information

### Polymorphism-Based Luminescence and Morphology-Dependent Optical Waveguide Property in the 1:1 Charge Transfer Cocrystals

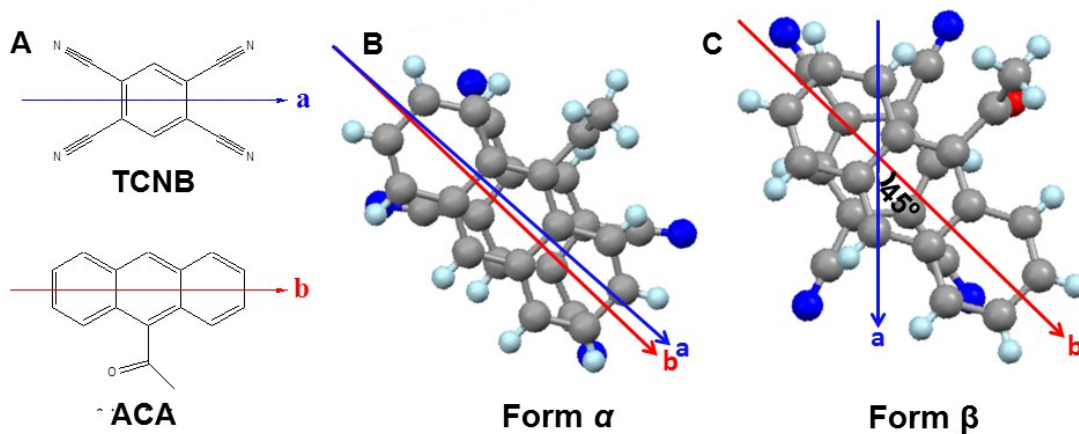
Jing Wang,<sup>\*a,b</sup> Shuping Xu,<sup>c</sup> Aisen Li,<sup>c</sup> Lei Chen,<sup>a,b</sup> Weiqing Xu<sup>\*c</sup> and Hongyu Zhang<sup>c</sup>

**Table S1** The Crystallographic data of form  $\alpha$  and form  $\beta$  cocrystals derived from single-crystal X-ray diffraction measurements.

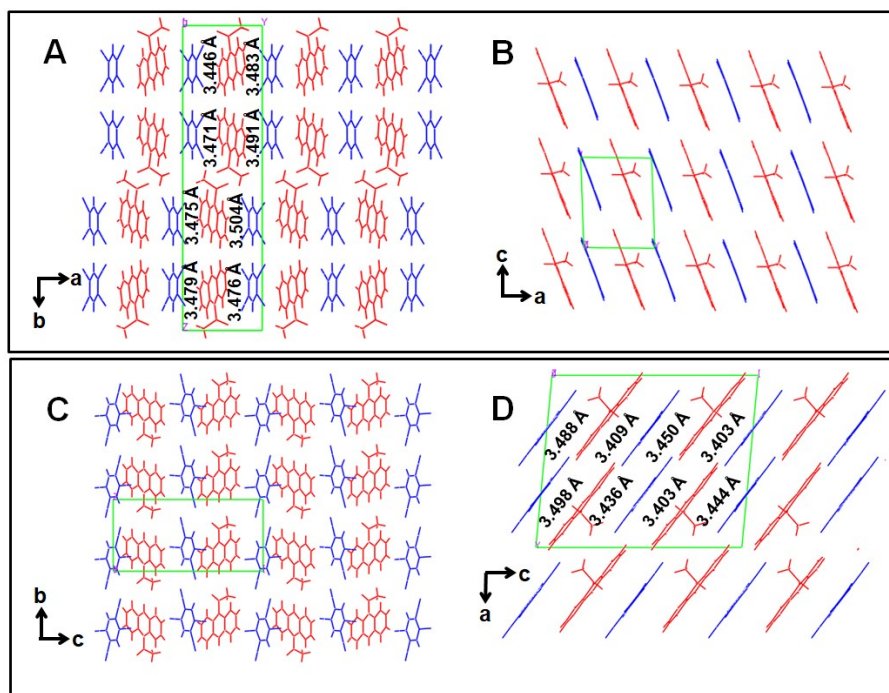
<b>Crystal</b>	<b>form <math>\alpha</math></b>
<b>Formula</b>	C <sub>26</sub> H <sub>14</sub> N <sub>4</sub> O
<b>Formula weight( g/mol)</b>	398.41
<b>Crystal system</b>	monoclinic
<b>Space-group</b>	P 21/c
<b>Lattice parameter a (Å)</b>	7.4866(4)
<b>Lattice parameter b (Å)</b>	28.6968(18)
<b>Lattice parameter c (Å)</b>	9.5251(6)
<b>cell parameter <math>\alpha</math>(°)</b>	90
<b>Lattice parameter <math>\beta</math>(°)</b>	92.720(3)
<b>Lattice parameter <math>\gamma</math>(°)</b>	90
<b>Cell volume (Å<sup>3</sup>)</b>	2044.1(2)
<b>Formula units per cell Z</b>	4
<b>Calculated density (g•cm<sup>-3</sup>)</b>	1.295
<b>Mu(mm<sup>-1</sup>)</b>	0.082
<b>F(000)</b>	824.0
<b>F(000)'</b>	824.31
<b>h,k,l,(max)</b>	9, 35, 11
<b>Nref</b>	4172
<b>R reflections</b>	0.0481(2653)
<b>wR2</b>	0.1196
<b>CSD</b>	NAFJIR



**Fig. S1** The intermolecular interactions of (a-c) form  $\alpha$  and (d-f) form  $\beta$  cocrystals.



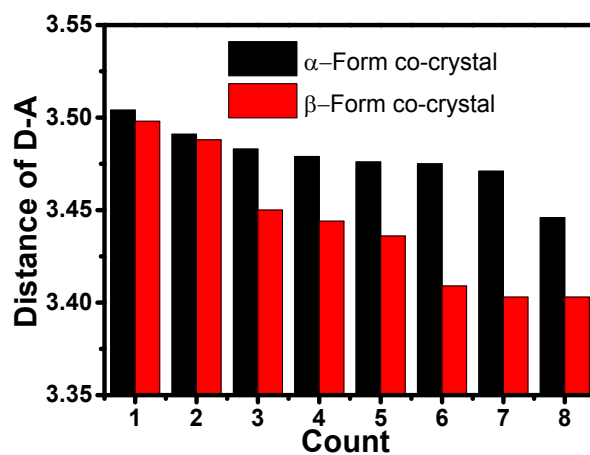
**Fig. S2** (A) Directions of ACA (marked as a) and TCNB (marked as b) are marked by arrowhead with different color. The Intermolecular  $\pi$ - $\pi$  interaction of ACA and TCNB with different rotation angles in (B) form  $\alpha$  and (C) form  $\beta$  cocrystals.



**Fig. S3** The interplanar distances between ACA and TCNB in the (A and B) form  $\alpha$  and (C and D) form  $\beta$  cocrystals.

**Table S2** The interplanar distances between ACA and TCNB in the form  $\alpha$  and form  $\beta$  from Fig. S3

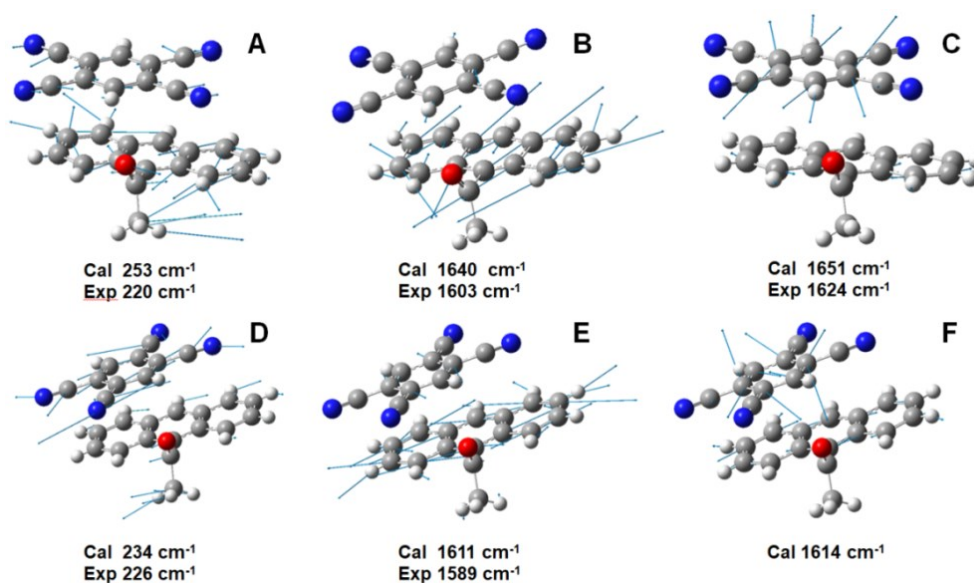
Crystal	$d_{D-A}$ (Å)	mean distance (Å)
form $\alpha$	3.504, 3.491, 3.483, 3.479, 3.476, 3.475, 3.471, 3.446	3.478
form $\beta$	3.498, 3.488, 3.450, 3.444, 3.436, 3.409, 3.403, 3.403	3.441



**Fig. S4** The Histogram of interplanar distances between ACA and TCNB in form  $\alpha$  (Black) and form  $\beta$  (Red) cocrystals from Table S2.

**Table S3** Intermolecular hydrogen bond interactions in form  $\alpha$  and form  $\beta$ .

Crystal Intermolecular interactions	form $\alpha$		form $\beta$	
	C-H...X (X = O, N)	Length of C-H...X	C-H...X (X = O, N)	Length of C-H...X
Interactions of ACA and adjacent ACA	C <sub>26</sub> -H <sub>26A</sub> ...O <sub>1</sub>	3.640 Å	C <sub>17</sub> -H <sub>17</sub> ...O <sub>1</sub> ;	2.503 Å
	C <sub>26</sub> -H <sub>26B</sub> ...O <sub>1</sub>	2.931 Å	C <sub>19</sub> -H <sub>19</sub> ...O <sub>1</sub>	2.539 Å
Interactions of TCNB and adjacent TCNB	C <sub>3</sub> -H <sub>3</sub> ...N <sub>4</sub>	2.581 Å	C <sub>3</sub> -H <sub>3</sub> ...N <sub>3</sub>	2.684 Å
	C <sub>3</sub> -H <sub>3</sub> ...N <sub>2</sub>	2.833 Å	C <sub>6</sub> -H <sub>6</sub> ...N <sub>2</sub>	2.706 Å
Interactions of TCNB with stacking ACA	C <sub>6</sub> -H <sub>6</sub> ...O <sub>1</sub>	2.603 Å	C <sub>6</sub> -H <sub>6</sub> ...O <sub>1</sub>	2.794 Å
	C <sub>26</sub> -H <sub>26A</sub> ...O <sub>1</sub>	2.905 Å		

**Fig. S5** In-plane  $\pi$ - $\pi$  vibration between ACA and TCNB in the (A-C) form  $\alpha$  and (D-F) form  $\beta$ .**Table S4.** The fluorescent lifetime of the form  $\alpha$  at 570, 580 and 590 nm, respectively.

570nm		580 nm		590 nm	
Value(ns)	Rel %	Value(ns)	Rel %	Value(ns)	Rel %
6.73	9.88	7.37	9.66	9.16	15.23
18.72	90.12	18.75	90.04	19.25	84.77

**Table S5** The fluorescent lifetime of the form  $\beta$  at 590, 610 and 630 nm, respectively.

590nm		610 nm		630 nm	
Value(ns)	Rel %	Value(ns)	Rel %	Value(ns)	Rel %
14.04	5.56	11.07	4.43	9.16	5.24

56.06	94.44	55.48	95.57	56.01	94.76
-------	-------	-------	-------	-------	-------

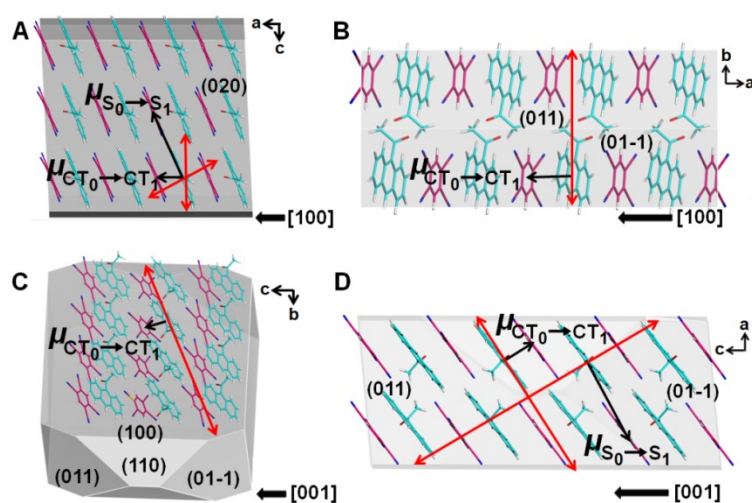


**Fig. S6** Transition dipole moments vector of  $CT_0$  to  $CT_1$  and  $S_0$  to  $S_1$  in the form  $\alpha$  viewed along the (A)  $[010]$ , (B)  $[001]$  directions, and that in form  $\beta$  viewed along the (C)  $[100]$ , (D)  $[010]$  directions, The vector  $\mu$  are marked as black single-headed arrows. The directions of the light propagation in the crystal are marked as red double-headed arrows. (A-D) Growth morphologies of the two forms are simulated using materials studio software.

The growth morphologies of the form  $\alpha$  and the form  $\beta$  polymorphic cocrystals were simulated via materials studio software. The ACA and TCNB molecules appear mixed stacking  $\cdots D-A-D-A \cdots$  along the direction of  $[100]$  in the form  $\alpha$  (Fig. S6A and S6B) and along the direction of  $[001]$  in the form  $\beta$  (Fig. S6C and S6D). Therefore, the form  $\alpha$  and the form  $\beta$  polymorphic cocrystals grow along the  $[100]$  and  $[001]$  directions, respectively.

The emitting light can travel around in the same plane which perpendicular to transition dipole moment ( $\mu$ ). Therefore, light propagation in the crystal were predicted by the vectors of  $\mu$  which from donor to acceptor. In the form  $\alpha$ , the composition vectors of  $\mu$  contain a  $CT_0$  to  $CT_1$  transition with parallel direction of the  $[100]$  and a  $S_0$  to  $S_1$  transition with an angle of  $\approx 60^\circ$  along the  $[100]$  direction (Black unfilled arrows represented the direction of  $\mu$  in the Fig. S6A and S6B), which lead to the optical wave can be transmitted along two directions of  $[001]$  and  $[100]$  with an angle of  $\approx 30^\circ$ . The directions of the light-wave propagation in form  $\beta$  are plotted in the Fig. S6C and S6D, the emitting light produced by  $CT_0$  to  $CT_1$  and  $S_0$  to  $S_1$

transitions can be travel in the crystal along the direction of [001] with an angle of  $\approx 60^\circ$  and  $30^\circ$ , respectively (Fig. S6C).

**Table S6** The distances of light propagation  $D_{b-t}$  and spatially resolved PL intensity from Fig. 4C.

No	$D_{b-t}$ (mm)	Fluorescent Intensity ( $I_{body}$ or $I_{tip}$ )
1	0	21926
2	0.15	8601
3	0.25	5248
4	0.4	1757
5	0.42	978
6	0.5	726
7	0.625	612
8	0.77	535
9	0.92	577
10	1.1	615
11	1.2	477

**Table S7** The distances of light propagation  $D_{b-t}$  and spatially resolved PL intensity from Fig. 4E.

No	$D_{b-t}$ (mm)	Fluorescent Intensity ( $I_{body}$ or $I_{tip}$ )
1	0	37246
2	0.15	21291
3	0.2	7119
4	0.25	2134
5	0.35	1890
6	0.5	1158

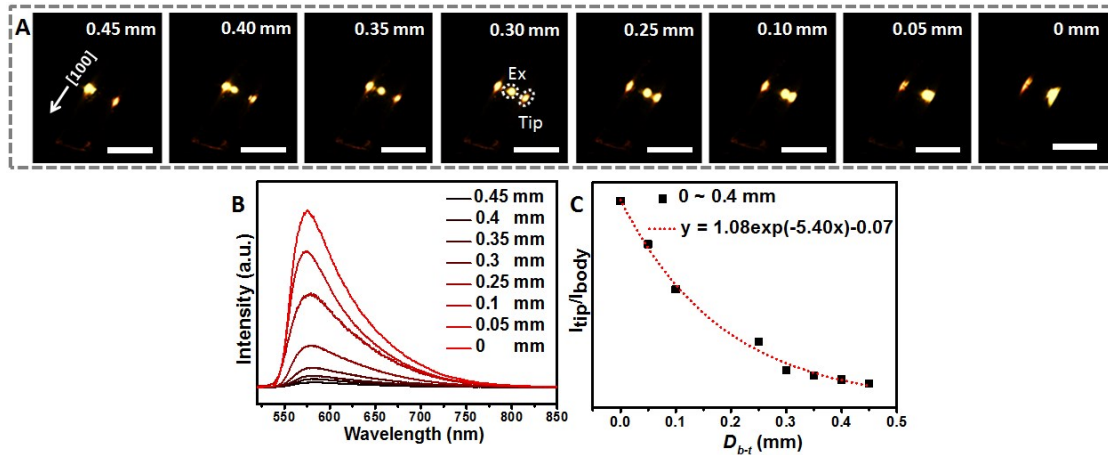


**Fig. S7** (A) PL micro-imagings of optical propagation in the form  $\alpha$ , the excitation spot moved perpendicular to the [100] axis (marked as 0.45 to 0 mm), white scale bars are 0.5 mm; (B) Spatially resolved PL spectra of out-coupled lights at the location of "Tip" in form  $\alpha$  from Fig. 7SA; (C) The fitting curves of  $I_{tip}/I_{body}$  with  $D_{b-t}$  from Fig. 7SB.

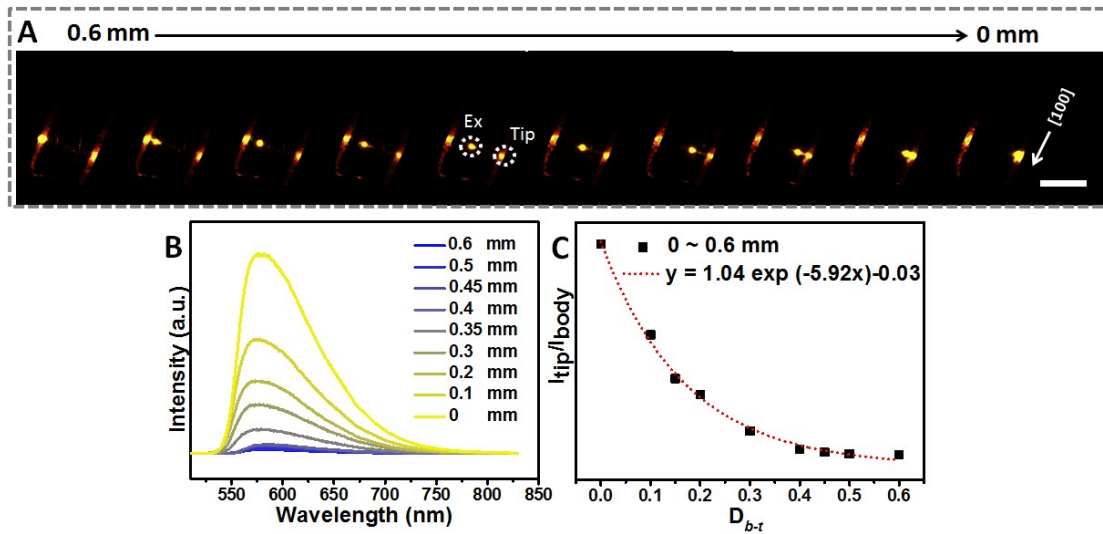


**Fig. S8** (A) PL micro-imagings of optical propagation in the form  $\alpha$ , the excitation spot moved perpendicular to the [100] axis (marked as 0.6 to 0 mm), white scale bar is 0.5 mm; (B) Spatially resolved PL spectra of out coupled lights at the location of “Tip” in form  $\alpha$  from Fig. 8SA; (C) The fitting curves of  $I_{\text{tip}}/I_{\text{body}}$  with  $D_{b-t}$  from Fig. 8SB.

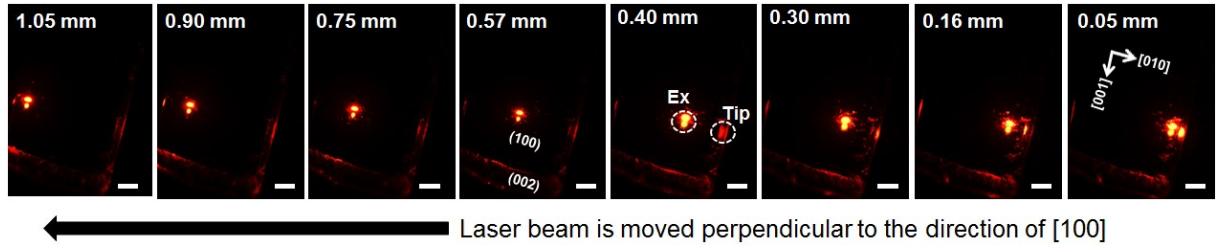


**Fig. S9** PL micro-imagings of form  $\beta$ , the incident laser beam from crystal tip to crystal body perpendicular the [001] axis with different distance  $D_{b-t}$ . The white scale bar is 0.25 mm.